

The definitive version is available at <http://onlinelibrary.wiley.com/>

## An Intercomparison Study of the Germanium Isotope Composition of Geological Reference Materials

Raphaëlle Escoube<sup>1,2</sup>, Olivier J. Rouxel<sup>2,3,4,\*</sup>, Béatrice Luais<sup>5</sup>, Emmanuel Ponzevera<sup>4</sup>,  
 Olivier F.X. Donard<sup>2</sup>

<sup>1</sup> LCABIE, U. Pau et Pays de l'Adour, CNRS UMR 525, Hélioparc 64053 Pau, France

<sup>2</sup> UEB-UBO, European Institute for Marine Studies IUEM, 29280 Plouzané, France

<sup>3</sup> Marine Chemistry and Geochemistry Department, Woods Hole Oceanographic Institution, Woods Hole, MA 02543, USA

<sup>4</sup> IFREMER, Centre de Brest, DRO/GM, 29280 Plouzané, France

<sup>5</sup> Centre de Recherches Péetrographiques et Géochimiques (CRPG) CNRS – UPR 2300, Nancy-Université, 15 rue Notre Dame des Pauvres, BP 20, 54501 Vandoeuvre-lès-Nancy Cedex, France

\*: Corresponding author : Olivier J. Rouxel, email address : [orouxel@ifremer.fr](mailto:orouxel@ifremer.fr)

### Abstract :

Recent analytical developments in germanium stable isotope determination by multicollector ICP-MS have provided new perspectives for the use of Ge isotopes as geochemical tracers. Here, we report the germanium isotope composition of the NIST SRM 3120a elemental reference solution that has been calibrated relative to internal isotopic standard solutions used in the previous studies. We also intercalibrate several geological reference materials as well as geological and meteoritic samples using different techniques, including online hydride generation and a spray chamber for sample introduction to MC-ICP-MS, and different approaches for mass bias corrections such as sample–calibrator bracketing, external mass bias correction using Ga isotopes and double-spike normalisation. All methods yielded relatively similar precisions at around 0.1‰ (2s) for  $\delta^{74/70}\text{Ge}$  values. Using igneous and mantle-derived rocks, the bulk silicate Earth (BSE)  $\delta^{74/70}\text{Ge}$  value was re-evaluated to be  $0.59 \pm 0.18\text{‰}$  (2s) relative to NIST SRM 3120a. Several sulfide samples were also analysed and yielded very negative values, down to  $-4.3\text{‰}$ , consistent with recent theoretical study of Ge isotope fractionation. The strong heavy isotope depletion in ore deposits also contrasts with the generally positive Ge isotope values found in many modern and ancient marine sediments.

### Résumé :

De récents développements analytiques ont permis la détermination de la composition isotopique du germanium par ICP-MS multi-collecteur, permettant de nouvelles perspectives dans l'utilisation des isotopes du germanium en tant que traceur géochimique. Dans ce papier, la composition isotopique du germanium de la solution de référence élémentaire NIST SRM 3120a a été calibrée par rapport aux standards utilisés dans les précédentes études. Différents matériaux de références ont été aussi intercalibrés ainsi que des échantillons géologiques et météoritiques en utilisant différentes techniques tels que l'introduction par génération d'hydrure en ligne et par chambre cyclonique, mais aussi différentes approches de correction de biais de masse tels que l'encadrement « échantillon-standard », l'utilisation d'un standard externe avec l'introduction de Ga et la normalisation par double spike. Toutes ces méthodes présentent des précisions relativement similaires autour de 0.1‰ (2s) pour la mesure du  $\delta^{74/70}\text{Ge}$ . A partir des roches ignées et dérivées du manteau, la valeur de  $\delta^{74/70}\text{Ge}$  de la terre silicatée globale (BSE) a été réévaluée autour de  $0.59 \pm 0.18\text{‰}$  (2s) par rapport au NIST SRM 3120a. Plusieurs échantillons de sulfures ont aussi été analysés et présentent des valeurs très négatives, jusqu'à  $-4.3\text{‰}$ , ce qui est consistant avec la récente étude théorique sur les fractionnements isotopiques du germanium. De plus, ce fort appauvrissement en isotope lourds dans les dépôts sulfurés contraste avec la tendance positive de la composition isotopique du germanium observée dans les sédiments marins actuels et passé.

**Keywords :** germanium ; Isotope ; Intercalibration ; reference materials

**Mots clés :** germanium ; Isotope ; Intercalibration ; matériaux de référence

## Introduction

Germanium (Ge) has 5 natural isotopes:  $^{70}\text{Ge}$ ,  $^{72}\text{Ge}$ ,  $^{73}\text{Ge}$ ,  $^{74}\text{Ge}$  and  $^{76}\text{Ge}$  with average relative isotope abundances of 20.84, 27.54, 7.73, 36.28 and 7.61 %, respectively. Early investigations of Ge isotopes using thermal ionization mass spectrometry (TIMS), SIMS and MC-ICP-MS were limited by an uncertainty of several per mil (Green *et al.* 1986, Hirata 1997, Shima 1964), mainly due to the presence of Ar-based interferences ( $\text{Ar}_2^+$  and  $\text{ArO}_2^+$ ) at  $m/z$  72, 74, 76, as well as interferences from  $^{70}\text{Zn}$  and  $^{76}\text{Se}$ . More recently, further analytical developments by MC-ICP-MS have permitted high precision Ge-isotope measurement with repeatability around 0.06 ‰ per mass unit (Galy *et al.* 2003, Luais 2003, 2007, Rouxel *et al.* 2006, Siebert *et al.* 2006, Yang and Meija 2010). Notably, Rouxel *et al.* (2006) and Siebert *et al.* (2006) applied a hydride generation (HG) technique coupled to MC-ICP-MS, which allow high-precision Ge-isotope analyses on natural samples for Ge amounts down to ~15 ng.

The analyses of Siebert *et al.* (2006) were done using a double spike approach while Rouxel *et al.* (2006) measured isotopic ratios and corrected for instrument fractionation with bracketing standards. In contrast, Luais *et al.* (2000) and Luais (2003, 2007) used a hexapole-collision cell MC-ICP-MS (Isoprobe GV Instrument) with  $\text{H}_2$  gas to remove  $\text{Ar}_2$  interferences, and corrected for instrument fractionation by using both Ga-isotopes as an internal normalization standard and by bracketing standards. Despite the obvious success in obtaining high precision measurement of Ge isotopes by MC-ICP-MS in a range of terrestrial and meteoritic materials, those previous studies have used a large diversity of techniques, standards, normalization ratios and instrumentations which preclude a straightforward comparison of published values. Thus, the concept of metrological traceability has not been applied.

Rouxel *et al.* (2006) obtained a crude estimate of the Ge isotopic composition of the Bulk Silicate Earth (BSE) by the analysis of various igneous rocks such as tholeiitic glasses from mid-ocean ridges, continental basalts and volcanic island basalts. Deep sea clays have  $\delta^{74}\text{Ge}$  values similar to BSE while modern deep-sea sponges and glauconite have  $\delta^{74}\text{Ge}$  values heavier than BSE. Considering that Ge isotope fractionation during biogenic opal and glauconite may favour enrichment in light isotopes in the forming product, it has been suggested that the Ge isotopic composition of the ocean is enriched in heavy isotopes relative to BSE (Rouxel *et al.* 2006). In addition, Mantoura (2006) carried out laboratory experiments indicating that cultured diatoms do not fractionate Ge isotopes. Luais (2003, 2007)

1  
2  
3 81 demonstrated that iron meteorites have a  $\delta^{74}\text{Ge}$  values heavier than terrestrial samples. The  
4  
5 82 homogeneous  $\delta^{74}\text{Ge}$  values for magmatic iron meteorites, regardless of their oxidation state  
6  
7 83 suggests, in agreement with experimental data (Luais et al., 2009), that core formation  
8  
9 84 processes do not fractionate significantly Ge isotopes in the metal phase with respect to the  
10  
11 85 primitive material, providing an estimate for Ge isotopic composition of the solar nebula.

12 86 Siebert et al. (2006) reported Ge isotope composition of hydrothermal waters collected  
13  
14 87 in the Oregon Cascades and in marine settings and found lighter isotope signatures relative to  
15  
16 88 basalts. However, a preliminary intercomparison performed by the authors and colleagues  
17  
18 89 suggests that the reported Ge-isotope compositions are plagued by calculating errors during  
19  
20 90 the data reduction scheme (C. Siebert, personal communication), precluding further  
21  
22 91 comparison with our study.

23 92 The aim of this paper is to compare analytical techniques to obtain Ge-isotope  
24  
25 93 composition of selected geological reference materials and to intercalibrate Ge-isotope  
26  
27 94 standards relative to the BSE estimate. We propose the use of a new reference material  
28  
29 95 NIST3120a to report natural Ge-isotope variations. This approach, together with further  
30  
31 96 studies of experimental and theoretical fractionation of Ge-isotopes (Galy *et al.* 2003, Luais et  
32  
33 97 al., 2009, Li *et al.* 2009, Li and Liu 2010) are essential steps toward the development of Ge-  
34  
35 98 isotopes as new geochemical tracer.

36 99

## 37 100 **Experimental procedures**

38  
39 101

### 40 41 102 *Reagents and Germanium standard solutions*

42 103 The hydride generation reagent is composed of 10 g of sodium borohydride powder  
43  
44 104 (high purity  $\text{NaBH}_4$ , Fisher Chemical) and 5 g of sodium hydroxide pellets (analytical grade  
45  
46 105  $\text{NaOH}$ , Acros Organics) dissolved into 1 l of ultra pure water (Milli-Q 18.2M $\Omega$ .cm,  
47  
48 106 Millipore), and is freshly prepared before each analytical session. During chemical  
49  
50 107 dissolution and purification, we used high purity  $\text{HNO}_3$  (distilled grade, CleanAcid, Analab)  
51  
52 108 and HF (optima grade, Fisher Chemical). Germanium standards used in this study include  
53  
54 109 NIST3120a (Lot #000411, 1000 $\mu\text{g/g}$ ); Spex (Lot #11-160GE); Aldrich (Lot #01704KZ;  
55  
56 110 Luais, 2000, Luais 2007), JMC (Johnson Matthey, Karlsruhe, Lot # 301230S; Luais 2007) and  
57  
58 111 Aristar (Lot # used in Rouxel et al., 2006 – incorrectly reported as Aldrich standard solution).  
59  
60 112 We also used Ga (Spex; Lot #12-98Ga; Cat # PLGA2-2Y) and Ga international isotopic  
113  
114 113 standard (NBS - SRM994, Lot# 680205, Luais et al., 2000; Luais 2007) prepared from Ga  
114  
114 114 metal as internal standards for instrumental mass bias corrections. Double Spike was prepared

1  
2  
3 115 from Ge metal spikes 73-70 from Isoflex USA Company (Ge-70 #32-01-70-3259 and Ge-73  
4 #32-01-73-1405). Each spike was dissolved separately in a mixture HNO<sub>3</sub>, sulfuric acid and  
5 116  
6  
7 117 trace HF and mixed to obtain a <sup>73</sup>Ge/<sup>70</sup>Ge ratio of ~ 0.6.  
8  
9 118

#### 10 119 *Geological reference materials and other geological samples*

11  
12 120 Several geological reference materials have been analyzed in this study for  
13 121 intercomparison purposes with previous studies by Rouxel et al. (2006). They include USGS  
14 122 standards (Govindaraju 1994) BHVO-2 (Hawaiian basalt), BIR-1 (Icelandic basalt), BCR-1  
15 123 (Basalt, Columbia River Group USA), G-2 (Granite, Rhode Island USA), GH (Granite,  
16 124 Hoggar, Algeria), DNC-1 (Braggtown Dolerite, North Carolina, USA), DTS-1 (Dunite,  
17 125 Hamilton, Washington), PCC-1 (Peridotite- a partially serpentinized harzburgite, California  
18 126 USA), AN-G (Anorthosite, Fiskenaeset, Western Greenland), GLO (Glauconite, Normandy  
19 127 France), and IF-G (Iron Formation, West Greenland).  
20  
21  
22  
23  
24  
25

26 128 We also analyzed the Iron meteorite Odessa (IAB group) for which Ge-isotope  
27 129 composition has been previously reported by Luais (2003, 2007). We also report Ge-isotope  
28 130 composition of hydrothermal sulfides (sphalerite) from volcanogenic sulfide deposits, the  
29 131 Navan Zn+Pb ore deposit in Ireland (Blakeman *et al.*, 2002), from continental hydrothermal  
30 132 ZnS ores from the St Salvy deposit in France (Luais, 2003, 2007), and from modern seafloor  
31 133 hydrothermal systems, the Lucky Strike field (Rouxel *et al.* 2004).  
32  
33  
34  
35  
36  
37  
38  
39

#### 40 135 *Sample dissolution and chromatographic separation*

41 136 A procedure adapted from Rouxel et al. (2006), Luais (2007) and Luais (submitted)  
42 137 was applied in this study for Ge purification from siliceous matrices, iron meteorites and  
43 138 sulfides. For HG-MC-ICP-MS method (IFREMER and WHOI laboratories), about 50 mg of  
44 139 siliceous material was dissolved in ~ 3 ml of 10 mol/l HF in a closed Teflon beaker on a hot  
45 140 plate at 70 °C and left to equilibrate overnight with an appropriate addition of double spike  
46 141 (spike/natural ratio ~ 1). After appropriate dilution to 1 mol/l HF with ultrapure water, the  
47 142 solution was directly purified without evaporation through a chromatographic column  
48 143 containing 2 mL of anion exchange resin (AG1-X8 Resin; 100-200 mesh; Chloride Form; Cat  
49 144 # 140-1441). The column is cleaned with several washes of 5 ml of 0.28 mol/l HNO<sub>3</sub>, distilled  
50 145 3 mol/l HNO<sub>3</sub>, and ultrapure water. After conditioning with 5 ml of 1 mol/l HF, the sample  
51 146 was loaded on the column and germanium strongly adsorbed on the resin. Matrix elements  
52 147 such Ca, Fe, Si or Zn were eluted and the resin further cleaned with 5 ml of 1 mol/l HF  
53 148 followed by 3 ml of ultrapure water. Ge was then eluted with 10 ml of 3 mol/l HNO<sub>3</sub> and the  
54  
55  
56  
57  
58  
59  
60

1  
2  
3 149 solution evaporated slowly to dryness on a hot plate. The final residue was dissolved in 3 ml  
4  
5 150 of 0.28 mol/l HNO<sub>3</sub> and ready for isotope analysis. Since the HG sample introduction system  
6  
7 151 allow complete separation of volatile Ge hydride from the aqueous sample matrix (e.g.  
8  
9 152 Rouxel et al., 2006), no further purification using cation exchange resin is required.  
10  
11 153 Procedures for iron meteorite and sulfide dissolution are detailed in Luais et al. (2000) and  
12  
13 154 Luais (2007). Briefly, it consists of dissolution using 2 mol/l and 14 mol/l HNO<sub>3</sub>,  
14  
15 155 respectively, followed by Ge isolation using AG50X8 cation exchange resin with 0.5 mol/l  
16  
17 156 HNO<sub>3</sub>. Procedures for silicate matrices used at CRPG (Luais, submitted) consist of HNO<sub>3</sub> +  
18  
19 157 HF dissolution followed by several steps of HF leaching to isolate Ge ( $\pm$  matrix) in the  
20  
21 158 supernatant. After evaporation and subsequent dissolution in 1 mol/l HF, an aliquot of the  
22  
23 159 sample is loaded on a AG1X8 anion exchange resin. Most of the remaining matrix is eluted  
24  
25 160 with 1 mol/l HF, and Ge is subsequently collected using 0.2 mol/l HNO<sub>3</sub>. Purification of Ge is  
26  
27 161 then performed on AG50X8 cationic resin similarly developed for iron meteorite matrix. The  
28  
29 162 efficiency of these procedures including 100 % yield and no isotopic fractionation during all  
30  
31 163 steps of Ge chemistry is demonstrated by Ge isotopic measurements of various matrices  
32  
33 164 doped with Ge standard, as well as Ge standard solutions after column separation. Details are  
34  
35 165 given in Luais (2007) for iron meteorite matrix and in Luais (submitted) and Rouxel et al.  
36  
37 166 (2006) for various silicate matrices from ultra-mafic, mafic to granitic in composition. In all  
38  
39 167 cases, the Ge isotopic composition of these Ge-doped matrices is similar within error to the  
40  
41 168 measured Ge standard solution.

169

#### 170 *MC-ICP-MS isotope ratio measurements:*

171 Germanium isotopes ratios were determined with a Thermo *Neptune* (Thermo Fisher  
172 Scientific; Waltham, MA, USA) at the Pôle Spectrométrie Océan (PSO, Brest) at IFREMER  
173 (Plouzané, France) and WHOI (Woods Hole, USA) using the hydride generation technique  
174 described by Rouxel *et al.* (2006). Pure standard solution and purified sample measurements  
175 were also performed on a Nu Plasma MC-ICP-MS at LCABIE laboratory (Pau, France) and  
176 Isoprobe (GV) MC-ICP-MS at CRPG laboratory (Nancy, France) (Luais 2007). The Neptune  
177 at WHOI and IFREMER was operating at low-mass resolution mode and <sup>70</sup>Ge, <sup>72</sup>Ge, <sup>73</sup>Ge  
178 and <sup>74</sup>Ge were measured on L2, C, H1, and H2 cups while <sup>68</sup>Zn, <sup>69</sup>Ga, <sup>71</sup>Ga and <sup>77</sup>Se were also  
179 monitored on L4, L3, L1 and H4 cups. The isotope <sup>76</sup>Ge was not measured due to a major  
180 interference of <sup>38</sup>Ar<sub>2</sub>. For the Nu plasma measurements at LCABIE, we set the cups as H6,  
181 H4, H2, and L2 for 74, 73, 72 and 70 at low mass resolution and the Ax and L3 cups for 71  
182 and 69 Ga isotopes. For the GV Isoprobe measurements (CRPG), <sup>70</sup>Ge, <sup>72</sup>Ge, <sup>73</sup>Ge and <sup>74</sup>Ge

1  
2  
3 183 were measured on Ax, H2, H3 and H4 cups while  $^{68}\text{Zn}$ ,  $^{69}\text{Ga}$ , and  $^{71}\text{Ga}$  were measured on L3,  
4  
5 184 L2, and H1 cups.

6  
7 185 Several introduction systems were used and include: (1) a cyclonic spray chamber  
8  
9 186 (SiS) equipped with PTFE micro concentric nebuliser at 50  $\mu\text{l}/\text{min}$  for WHOI, IFREMER and  
10  
11 187 CRPG (Luais 2007) while a Quartz micro concentric nebuliser at 100  $\mu\text{l}/\text{min}$  was used for  
12  
13 188 LCABIE measurements; (2) continuous flow hydride generation systems, CETAC HGX-200  
14  
15 189 at WHOI and IFREMER (see Rouxel *et al.*, 2006 for instrument settings) and a custom-built  
16  
17 190 HG generator at the LCABIE.

18  
19 191 Instrumental mass bias was corrected using several techniques as described in  
20  
21 192 previous studies (Galy *et al.* 2003, Luais 2007, Rouxel *et al.* 2006, Siebert *et al.* 2006): (1) a  
22  
23 193 sample-standard bracketing (referred to as SSB) technique that involves the measurement of  
24  
25 194 the Ge standard solution, before and after each unknown sample (Galy *et al.* 2003, Rouxel *et*  
26  
27 195 *al.* 2006); (2) external normalization to Ga-isotopes (referred as Ga-Cor) (Galy *et al.* 2003,  
28  
29 196 Hirata 1997, Luais *et al.* 2000, Luais 2007, Siebert *et al.* 2006) and Cu-isotopes. (3) Double  
30  
31 197 spike (DS) correction ( $73/70$ ) was performed as described by Siebert *et al.* (2006). The double  
32  
33 198 spike solution was mixed with the sample before chemical purification with a spike/natural  
34  
35 199 ratio of around 1 (g/g). Data reduction of Ge-isotope ratios was performed using a scheme  
36  
37 200 similar to Siebert *et al.* (2001). In some cases, we coupled the hydride generation system with  
38  
39 201 the regular cyclonic spray chamber using an extra inlet available on the spray chamber. This  
40  
41 202 approach allowed a direct comparison of instrumental mass bias induced by both techniques  
42  
43 203 and the calculation of hydride generation yield. It also permitted the use of Ga as an internal  
44  
45 204 standard to correct for instrumental mass bias during hydride generation.

46 205

## 47 206 **Results and discussion**

48 207

### 49 208 *Notation and data normalization*

50 209 Germanium isotope composition can be reported using several possible notations, such as:

51 210

$$52$$

$$53$$

$$54 \quad 211 \quad \delta^x\text{Ge} (\text{‰}) = \left( \frac{({}^x\text{Ge}/{}^{70}\text{Ge})_{\text{sample}}}{({}^x\text{Ge}/{}^{70}\text{Ge})_{\text{STD}}} - 1 \right) \times 1000 \quad (1)$$

$$55$$

$$56$$

57 212

58  
59 213 Where  $x = 74, 73$  or  $72$  and STD corresponds to the normalization to Ge-standard.

60 214 Currently, there is no consensus in the way to report Ge-isotope ratios. Siebert *et al.* (2006)

1  
2  
3 215 reported  $\delta^{74/72}\text{Ge}$  due to the double spike correction using  $^{73}\text{Ge}$  and  $^{70}\text{Ge}$  spikes. Galy *et al.*  
4  
5 216 (2003) reported  $\delta\text{Ge}$  per mass unit while Rouxel *et al.* (2006) and Luais (2003, 2007) reported  
6  
7 217  $\delta^{74/70}\text{Ge}$  (together with other 73/70 and 72/70 isotope ratios). Due to larger abundances and  
8  
9 218 minor isobaric interferences, the  $^{74}\text{Ge}/^{70}\text{Ge}$  ratio seems to be optimum for reporting Ge-  
10  
11 219 isotopes. Throughout this study, we reported  $\delta^{74}\text{Ge}/^{70}\text{Ge}$  values relative to SRM3120a which  
12  
13 220 is a concentration standard produced in large amount.  
14  
15 221

#### 16 222 *Isobaric interferences and instrumental mass bias*

17 223 Ge isotope measurements suffer from molecular interferences, such as  $^{35}\text{Cl}^{35}\text{Cl}^+$  on  
18 224  $^{70}\text{Ge}^+$ ;  $^{40}\text{Ar}^{16}\text{O}_2^+$  and  $^{36}\text{Ar}^{36}\text{Ar}^+$  on  $^{72}\text{Ge}^+$ ,  $^{58}\text{Ni}^{16}\text{O}^+$  and  $^{38}\text{Ar}^{36}\text{Ar}^+$  on  $^{74}\text{Ge}^+$  and  $^{38}\text{Ar}^{38}\text{Ar}^+$  and  
19 225  $^{36}\text{Ar}^{40}\text{Ar}^+$  on  $^{76}\text{Ge}^+$ . On the Neptune and Nu Plasma coupled to HG, those interferences are  
20  
21 226 minimized and are generally negligible except for  $^{76}\text{Ge}$ , as previously discussed by Rouxel *et*  
22  
23 227 *al.* (2006). We however observed a ubiquitous interference on  $^{70}\text{Ge}^+$  during the early stage of  
24  
25 228 analytical development on the Neptune, probably from  $^{40}\text{Ar}^{14}\text{N}^{16}\text{O}$  due to the use of X-cones  
26  
27 229 which may induce a higher oxide-level. Therefore, we only used normal cones throughout this  
28  
29 230 study. On the GV Isoprobe, hydrogen addition in the hexapole collision cell was used to  
30  
31 231 remove  $\text{Ar}_2$  interferences (Luais *et al.* 2000; Luais, 2007).  
32

33 232 Ge-isotope measurements, and in particular double-spike correction, may suffer from  
34 233 potential  $\text{GeH}^+$  interference. Therefore, we evaluated the contribution of  $^{70}\text{GeH}^+$  on mass 71  
35 234 by measuring  $(^{71}\text{Ga}^+ + ^{70}\text{GeH}^+)/^{69}\text{Ga}^+$  ratios. This approach permits us to evaluate the influence  
36  
37 235 of  $\text{GeH}^+$  on the signal, which is around 0.001 ‰ and thus negligible, in agreement with  
38  
39 236 Luais *et al.* (2000).  
40

41 237 Isotopic measurements on all instruments were also corrected for Zn interferences on  
42  
43 238 mass 70 using  $^{68}\text{Zn}$ , with a mass bias applied on  $^{70}\text{Zn}/^{68}\text{Zn}$  ratios (Luais, 2007).  
44

45 239 As germane ( $\text{GeH}_4$ ) formation in the hydride generator may induce isotope  
46  
47 240 fractionation, we coupled the spray injection system with the HG to evaluate potential mass  
48  
49 241 bias. This analytical setup allowed a direct comparison of the Ge-isotope ratios of the  
50  
51 242 standard introduced using conventional spray chamber (“Standard”) vs. hydride generation  
52  
53 243 (“Sample”) (Figure 1). The SRM3120a Ge standard solution was adjusted to a concentration  
54  
55 244 of 250 ng/g for spray chamber injection and to 10 ng/g for hydride generation to reach similar  
56  
57 245 intensity for both introduction systems. The results suggest that the difference in mass bias  
58  
59 246 between the spray chamber and the HG system is about 0.05 +/- 0.07 ‰ (2s) per mass unit,  
60  
247 which suggest that, either Ge-hydride formation does not fractionate Ge-isotopes or that the  
248 hydride formation yield is quantitative. Considering that the spray chamber system has an

1  
2  
3 249 efficiency of Ge transfer into the plasma torch of about 20 % (determined using the volume of  
4  
5 250 solution taken vs. solution drained in waste), we can determine an overall sensitivity in  
6  
7 251 abundance of 0.85 pg/V. In comparison, we calculate that hydride generation has a sensitivity  
8  
9 252 of 0.91 pg/V which suggest that about 100% of germanic acid in solution is reduced to  
10  
11 253 germane species.

12 254

#### 13 14 255 *Assessment of standard and double-spike isotope composition*

15 256 While Ga is traditionally used to control the mass bias for Ge analyses (Galy *et al.*  
16 257 2003, Hirata 1997, Luais *et al.* 2000, Luais 2007,), we recognize that such approach may not  
17  
18 258 allow absolute Ge isotope ratio measurement since instrumental mass bias may be different  
19  
20 259 between elements (e.g. Maréchal *et al.* 1999, Yang and Meija 2010, Meija *et al.* 2009). We  
21  
22 260 however found that Ga or Cu can be appropriate elements for external mass bias correction  
23  
24 261 and determination of relative isotopic composition (in delta value) of Ge standards or  
25  
26 262 samples. The assumption of identical mass bias for analyte and standard however require  
27  
28 263 identical matrix composition and concentrations. In addition, external mass bias correction  
29  
30 264 yields identical results in delta values than standard-sample bracketing method or double  
31  
32 265 spike normalization, as presented in Tables 2 and 3 and discussed below.

33 266 The double-spike composition was defined relative to the NIST 3120a composition  
34  
35 267 obtained on the Neptune at PSO, Brest (Table 1) using conventional spray chamber  
36  
37 268 introduction system. In order to calibrate the Ge-isotope ratios of NIST 3120a, we used a  
38  
39 269 Gallium standard solution (Spex; Lot #12-98Ga) to correct for instrumental mass bias using  
40  
41 270  $^{69}\text{Ga}/^{71}\text{Ga}$  ratio of 1.50676 (Machlan *et al.*, 1986). This approach was also used to monitor  
42  
43 271 instrumental mass bias between analyses of pure standard and double spike. It is important to  
44  
45 272 note that both our double spike and NIST 3120a calibration reported in Table 1 may differ  
46  
47 273 from the *true* value but this potential bias does not affect the final isotope ratios when using  
48  
49 274 the delta notation. Although we didn't determine the optimum double spike composition or  
50  
51 275 spike/natural ratios using error propagation tests, Figure 2 shows that spike/natural ratio  
52  
53 276 between 0.8 to 3.5 yield consistent results with overall precision of 0.15 ‰ (2s). In practice, a  
54  
55 277 ratio between 1 to 2 was routinely used for isotope analysis. This optimal ratio is very similar  
56  
57 278 to the one used by Siebert *et al.* (2006).

58 279

#### 59 280 *Intercomparison of Ge isotope compositions of Ge standard solutions*

60 281 The average compositions of NIST3120a and other standard solutions over multiple  
282 analytical sessions for different instruments and measurement setups are reported in Table 2.



1  
2  
3 283 *Aristar* and *Spex* solutions show an enrichment in the light isotope of approximately the same  
4 proportion ( $\delta^{74/70}\text{Ge} = -0.64 \pm 0.18 \text{ ‰}$  (2s) and  $-0.71 \pm 0.20 \text{ ‰}$  (2s), respectively). *JMC*  
5 284 standard also presents an enrichment in the light isotope although in smaller proportion, with  
6 a  $\delta^{74/70}\text{Ge}$  value of  $-0.32 \pm 0.10 \text{ ‰}$  (2s). The *Aldrich* standard shows the lightest  $\delta^{74/70}\text{Ge}$   
7 285 values at  $-2.01 \pm 0.22 \text{ ‰}$  (2s). Several sample introduction systems were tested, using either  
8 286 spray chamber (SiS) or hydride generation (HG) for different instruments (Neptune, Nu  
9 287 plasma or Isoprobe) and no systematic differences were found. It is also important to note that  
10 288 standard-sample bracketing, Ga normalization and double spike corrections yielded similar  
11 289 results, both in terms of Ge isotope composition and analytical precision.  
12  
13  
14  
15  
16  
17  
18  
19  
20

### 21 293 *Ge isotope composition of geochemical RM and re-evaluation of the bulk silicate Earth value*

22  
23 294 Selected geochemical RM, measured using double spike (this study), sample-standard  
24 295 bracketing (Rouxel *et al.* 2006), and Ga normalization (Luais 2007) methods are reported in  
25 296 Table 3. In addition, we report precise Ge concentrations determined by isotope dilution since  
26 297 the double spike data reduction scheme offers the advantage to also calculate precisely the Ge  
27 298 concentration of the samples.

28  
29  
30  
31 299 Based on these data, the bulk silicate Earth value has been re-evaluated as  $\delta^{74/70}\text{Ge} =$   
32 300  $0.56 \text{ ‰}$  versus NIST SRM3120a. This average is determined from igneous rocks (BHVO-2;  
33 301 BIR-1; BCR-1) having limited variations (2s = 0.08 ‰). Granitic rocks display significant  
34 302 deviation from the bulk silicate Earth with G-2 (Rhode Island, USA) having a slightly lighter  
35 303 composition at  $0.40 \pm 0.04 \text{ ‰}$  (2s). Ultramafic rocks, although less concentrated in Ge,  
36 304 present similar compositions as basaltic rocks. We note that NIST3120a is the standard whose  
37 305 isotope composition is the closest to the BSE relative to the other standard solutions used  
38 306 previously (Table 2). As discussed below, iron formation IF-G and marine sediment GL-O  
39 307 yield heavier  $\delta^{74/70}\text{Ge}$  values at  $1.03 \pm 0.10 \text{ ‰}$  (2s) and  $2.44 \pm 0.14 \text{ ‰}$  (2s) respectively.  
40  
41  
42  
43  
44  
45  
46  
47

48 308 Although Ge concentrations have been widely reported in geochemical reference  
49 309 materials (Govindaraju 1994), they are only rarely analyzed by isotope dilution and even  
50 310 more rarely by MC-ICP-MS after chemical purification. In most cases, our new concentration  
51 311 data in Table 3 are within 5% of previously reported data (e.g. BIR-1, BCR-1, G-2, DNC-1,  
52 312 AN-G, IF-G) while differences may be up to 10-20% in some cases (e.g. GH, DTS-1, PCC-1,  
53 313 GL-O).  
54  
55  
56  
57  
58  
59  
60

### 315 *Ge isotope composition of meteorites, sediments and sulfide deposits*

1  
2  
3 316 As shown in **Figure 3**, the absolute range of  $\delta^{74/70}\text{Ge}$  values in rocks and minerals is  
4  
5 317 about 8.05‰ which is comparable or even larger than most non traditional stable isotope  
6  
7 318 systems (e.g. Anbar and Rouxel 2007). The strong heavy isotope depletion in sulfides  
8  
9 319 contrasts strongly with the generally positive Ge isotope values found in many modern and  
10  
11 320 ancient marine sediments (e.g. banded iron formations, glauconite).

12 321 Glauconite (GLO) and Iron Formation (IF-G) are two iron-rich rocks where redox  
13  
14 322 conditions were important in their formation. Glauconite is a secondary clay mineral which is  
15  
16 323 formed in marine sediments during the reduction of Fe(III) to Fe(II), while Archean Iron  
17  
18 324 Formation is believed to have formed in globally anoxic oceans where hydrothermal Fe(II)  
19  
20 325 was partially oxidized and co-precipitated with silica, either biotically or abiotically (e.g.  
21  
22 326 Bekker *et al.*, 2010). In both deposit types, Ge is enriched relative to crustal values with  
23  
24 327 Ge/Si ratios of  $6.44 \times 10^{-6}$  and  $2.7 \times 10^{-5}$  mol/mol for Glauconite and Iron formation,  
25  
26 328 respectively. Since Galy *et al.* (2002) and Li and Liu (2010) suggested that Ge adsorbed onto  
27  
28 329 iron oxyhydroxide is enriched in light isotopes, the positive  $\delta^{74/70}\text{Ge}$  values for GLO and IF-G  
29  
30 330 is best explained by the heavy isotope composition of their Ge sources. In this case, the  
31  
32 331 slightly lighter values for IF-G may potentially result from the contribution of hydrothermal  
33  
34 332 Ge to Archean oceans (Hamade *et al.* 2003). Further studies are however required to address  
35  
36 333 this issue.

37 334 Deep sea sponges of the NE Pacific (Rouxel *et al.* 2006) show an average isotope  
38  
39 335 composition at around 2.47 ‰. The relatively high  $\delta^{74/70}\text{Ge}$  values obtained for different  
40  
41 336 species at different depths also suggest that sponges likely record the Ge isotope composition  
42  
43 337 of seawater. This value is a lower bound of the Ge isotopic composition of modern seawater  
44  
45 338 because, if sponges fractionate Ge isotopes, they likely discriminate against heavy isotopes as  
46  
47 339 already observed for Si isotopes. More recently, Mantoura (2006) reported  $\delta^{74/70}\text{Ge}$  values for  
48  
49 340 cleaned diatom opal from Holocene sediments at around 3.3 ‰. Those results, together with  
50  
51 341 the lack of Ge isotope fractionation observed during Ge uptake by cultured diatoms  
52  
53 342 (Mantoura, 2006), further confirm that seawater is enriched in the heavy Ge isotopes,  
54  
55 343 probably close to 3 ‰.

56 344 Two independent Ge isotope analyses of the non-magmatic iron meteorite Odessa are  
57  
58 345 reported in Table 4 and are in perfect agreement. Also is reported the recalculated Ge isotopic  
59  
60 346 composition of the magmatic iron meteorite Braunau (IIA). It is worthwhile to note that the  
347 Ge isotope composition of various types of iron meteorites (magmatic and non-magmatic  
348 irons) deviate from BSE in contrast to other heavy stable isotope systems (such as Cu, Zn, Fe;

1  
2  
3 349 Moynier *et al.* 2007), confirming the complexity of metal-silicate segregation and the  
4  
5 350 importance of volatilization/alteration effects (Luais, 2007).  
6

7 351 Both sphalerite from ancient Pb-Zn ore deposits (Blakeman *et al.* 2002) and seafloor  
8  
9 352 hydrothermal deposits at Lucky Strike (Rouxel *et al.* 2004) have been analyzed and an  
10  
11 353 average  $\delta^{74}\text{Ge}$  value of  $-3.53 \pm 0.51\text{‰}$  has been obtained (Table 4). Sphalerite from the single  
12  
13 354 ZnS ore deposit of St Salvy mine (France), precipitated from hydrothermal fluids related to  
14  
15 355 plutonic intrusion, also exhibit negative values with a range of -1 to -2 ‰ (Luais, 2007).  
16  
17 356 These results are interesting because Ge isotopes in sulfides are completely shifted toward  
18  
19 357 negative values by  $\sim 4\text{‰}$  relative to BSE. In contrast, preliminary Ge isotope analysis from  
20  
21 358 hydrothermal fluids yield variable  $\delta^{74}\text{Ge}$  values around  $1.9 \pm 0.5\text{‰}$  (Escoube *et al.* 2008,  
22  
23 359 Rouxel *et al.* 2008). The recent study by Li *et al.* (2009) estimating equilibrium fractionation  
24  
25 360 factors in the Ge isotope system suggested a very large fractionation toward lighter values (up  
26  
27 361 to  $10\text{‰}$  at  $25\text{ °C}$ ) in Ge-bearing sulfides relative to 4-coordinated Ge–O compounds (e.g.  
28  
29 362  $\text{Ge}(\text{OH})_4(\text{aq})$  or quartz). Therefore, the large difference between sulfides and BSE is best  
30  
31 363 explained by a strong isotopic fractionation (may be up to  $4.5\text{‰}$ ) during sulfide precipitation  
32  
33 364 in hydrothermal systems.  
34

### 35 365 36 366 **Conclusion**

37 367 This study permits an intercomparison of germanium isotope measurement techniques  
38  
39 368 as well as a calibration of several geological reference materials and mono-elemental standard  
40  
41 369 solutions used in previous studies. Different methodologies were used during this study: (1)  
42  
43 370 introduction by on-line hydride generation and spray chamber, and (2) mass bias correction  
44  
45 371 by sample-standard bracketing, external mass bias correction using Ga or Cu isotopes and  
46  
47 372 double spike normalization. Even if all methods yield consistent isotope composition with  
48  
49 373 similar precisions ( $2s \sim 0.15\text{‰}$ ), the double spike correction offers the advantage of providing  
50  
51 374 high-precision Ge concentrations and correcting for potential Ge isotope fractionation during  
52  
53 375 sample dissolution and purification.

54 376 Using igneous and mantle-derived rocks, the Bulk Silicate Earth (BSE) was re-  
55  
56 377 evaluated to  $0.59 \pm 0.18\text{‰}$  ( $2s$ ) relative to NIST3120a. In comparison, Iron meteorites  
57  
58 378 exhibit more positive values of  $\delta^{74/70}\text{Ge}$  up to  $+1.5\text{‰}$ . We report an overall  $\delta^{74/70}\text{Ge}$  variation  
59  
60 379 in terrestrial rocks and minerals of about  $8\text{‰}$ . This range is comparable or even larger than  
380  
381 380 most non-traditional stable isotope systems (e.g., Fe). This large range of compositions is  
mainly due to the extreme value (down to  $-4.3\text{‰}$ ) for sulfide samples originating from

1  
2  
3 382 hydrothermal environments, consistent with theoretical calculations (Li *et al.* 2009). This  
4  
5 383 strong isotope depletion in sulfides contrasts drastically with the generally positive Ge isotope  
6  
7 384 values found in many modern and ancient marine sediments (e.g. banded iron formations,  
8  
9 385 glauconite). Large variation in germanium stable isotopes and their reproducible measurement  
10  
11 386 provides new perspectives on the use of Ge as a novel geochemical tracer, in particular for  
12  
13 387 tracing planetary and oceanic processes.  
14  
15 388  
16 389

### 17 390 **Acknowledgements**

19 391 This study was supported by the Woods Hole Oceanographic Institution, Europole  
20  
21 392 Mer, UEB, UBO, IFREMER and CRPG Nancy (INSU-PNP). Lary Ball (WHOI), Jurek  
22  
23 393 Blustajn (WHOI), Maureen Auro (WHOI), Yoan Germain (IFREMER), Sylvain Bérail  
24  
25 394 (LCABIE) and Delphine Yeghicheyan (SARM-CRPG-Nancy) are thanked for their technical  
26  
27 395 support. We thank Stefan Lalonde, Thomas Meisel and two anonymous reviewers for helpful  
28  
29 396 comments on the manuscript. Adrian Boyce and Yves Fouquet are thanked for providing  
30  
31 397 sulfide samples.  
32  
33 398  
34  
35  
36  
37  
38  
39  
40  
41  
42  
43  
44  
45  
46  
47  
48  
49  
50  
51  
52  
53  
54  
55  
56  
57  
58  
59  
60

1  
2  
3 399 **Figure Captions**  
4

5 400  
6  
7 401 Figure 1: (A) Comparison between hydride generation (HG) and spray chamber (SiS)  
8 402 methods for Ge isotope analysis. A NIST3120a solution was alternatively introduced through  
9 403 the HG (square), considered as an “unknown sample” at a concentration of 10 ng/g, and  
10 404 through the SiS (Diamond), used as “bracketing standard” at a concentration of 250 ng/g. The  
11 405 concentrations were adjusted to obtain the same voltage (graph A). (B) Ge isotope  
12 406 composition (in delta values) of the NIST3120a standard determined by HG and normalized  
13 407 to SiS values.  
14  
15  
16  
17  
18  
19  
20

21 409 Figure 2: Ge isotope composition of NIST3120a and Aldrich standards determined using a  
22 410 double spike method with different Spike/Sample ratios. While the addition of spike in  
23 411 proportions of 0.6-4 relative to sample yielded approximately stable  $\delta^{74}\text{Ge}$  values, analyses  
24 412 are best performed with Spike/Sample ratios between 1 and 2.  
25  
26  
27  
28  
29

30 414 Figure 3: Compilation of Ge isotope composition ( $\delta^{74/70}\text{Ge}$ ) of geological reference materials  
31 415 and natural samples versus NIST3120a; (a) Luais, 2007; (b) Rouxel et al., 2006; (c) this  
32 416 study; (d) Mantoura (2006).  
33  
34  
35  
36  
37  
38  
39  
40  
41  
42  
43  
44  
45  
46  
47  
48  
49  
50  
51  
52  
53  
54  
55  
56  
57  
58  
59  
60

1  
2  
3 418 **Table Captions**  
4

5 419

6  
7 420 Table 1: Ge isotope compositions of NIST3120a standard and Ge70-73 double spike  
8  
9 421 determined on the Neptune MC-ICP-MS after internal normalisation to Ga for instrumental  
10 422 mass bias correction  
11

12 423

13  
14 424 Table 2: Intercalibration of Ge isotope composition of standard solutions against NIST 3120a.  
15

16 425

17 426 Table 3: Intercomparison study of Ge isotope compositions of geochemical RM versus NIST  
18  
19 427 3120a.  
20

21 428

22  
23 429 Table 4: Ge isotope compositions of sulfides and iron meteorites.  
24  
25  
26  
27  
28  
29  
30  
31  
32  
33  
34  
35  
36  
37  
38  
39  
40  
41  
42  
43  
44  
45  
46  
47  
48  
49  
50  
51  
52  
53  
54  
55  
56  
57  
58  
59  
60

1  
2  
3 430 **References.**

4  
5 431  
6 432 **Anbar A.D. and Rouxel O. (2007)**  
7 433 Metal stable isotopes in paleoceanography. **Annual Review of Earth and Planetary**  
8 434 **Sciences**, 717-746.  
9 435

10 436 **Blakeman R.J., Ashton J.H., Boyce A.J., Fallick A.E. and Russell M.J. (2002)**  
11 437 Timing of interplay between hydrothermal and surface fluids in the Navan Zn + Pb ore body,  
12 438 Ireland: Evidence from metal distribution trends, mineral textures, and d34S analyses  
13 439 **Economic Geology**, 97, 73-91.  
14 440

15 441 **Chang T.-L., Li W.-J., Qiao G.-S., Qian Q.-Y. and Chu Z.-Y. (1999)**  
16 442 Absolute isotopic composition and atomic weight of germanium **International Journal of**  
17 443 **Mass Spectrometry**, 189, 205-211.  
18 444

19 445 **Escube R., Rouxel O. and Donard O.F.X. (2008)**  
20 446 Measurement of Germanium isotope composition in marine samples by hydride generation  
21 447 coupled to MC-ICP-MS. **Geophysical Research**, 10, abstract EGU2008-A-12035.  
22 448

23 449 **Galy A., Pokrovsky O.S. and Shott J. (2002)**  
24 450 Ge-isotope fractionation during its sorption on goethite: an experimental study **Geochemica**  
25 451 **et Cosmochimica Acta**, 66, A259.  
26 452

27 453 **Galy A., Pomiès C., Day J.A., Pokrovsky O.S. and Schott J. (2003)**  
28 454 High precision measurement of germanium isotope ratio variations by multiple collector-  
29 455 inductively coupled plasma mass spectrometry **Journal of Analytical Atomic Spectrometry**,  
30 456 **18**, 115-119.  
31 457

32 458 **Govindaraju K. (1994)**  
33 459 compilation of working values and sample description for 383 geostandards **Geostandards**  
34 460 **Newslett.**, 18, 1-158.  
35 461

36 462 **Green M.D., Rosman K.J.R. and De Laeter J.R. (1986)**  
37 463 The isotopic composition of germanium in terrestrial samples **International Journal of Mass**  
38 464 **Spectrometry and Ion Processes**, 68, 15-24.  
39 465

40 466 **Hamade T., Konhauser K.O., Raiswell R., Goldsmith S. and Morris R.C. (2003)**  
41 467 Using Ge/Si ratios to decouple iron and silica fluxes in Precambrian banded iron formations  
42 468 **Geology**, 31, 35-38.  
43 469

44 470 **Hirata T. (1997)**  
45 471 Isotopic variations of germanium in iron and stony iron meteorites **Geochimica et**  
46 472 **Cosmochimica Acta**, 61, 4439-4448.  
47 473

48 474 **Li X., Zhao H., Tang M. and Liu Y. (2009)**  
49 475 Theoretical prediction for several important equilibrium Ge isotope fractionation factors and  
50 476 geological implications **Earth and Planetary Science Letters**, 287, 1-11.  
51 477

52 478 **Li X.F. and Liu Y. (2010)**

- 1  
2  
3 479 First-principles study of Ge isotope fractionation during adsorption onto Fe(III)-  
4 480 oxyhydroxides surfaces **Chemical Geology**, **278**, 15-22.  
5 481  
6  
7 482 **Luais B. (2007)**  
8 483 Isotopic fractionation of germanium in iron meteorites: Significance for nebular condensation,  
9 484 core formation and impact processes **Earth and Planetary Science Letters**, **262**, 21-36.  
10 485  
11 486 **Luais B., Framboisier X., Carignan J., and Ludden J. (2000)** Analytical development of  
12 487 Ge isotopic analyses using multi-collection plasma source mass spectrometry: Isoprobe MC-  
13 488 Hex-ICP-MS (Micromass). **Geoanalysis 2000**, Pont-à-Mousson, France, 45-46.  
14 489  
15 490  
16 491 **Luais B. (2003)**. Germanium isotope systematics in Meteorites. **Meteorit. Planet. Sci.**, **38**,  
17 492 A31.  
18 493  
19 494 **Luais B., Toplis M.J., Tissandier L., Roskosz M. (2009)**  
20 495 Metal-silicate segregation and fractionation of Ge isotopes : comparison with experimental  
21 496 data and meteorites, **Meteorit. Planet. Sci.** **44**, **7**, A124.  
22 497  
23 498 **Machlan, L.A., Gramlich, J.W., Powell, L.J., Lambert, G.M. (1986)**  
24 499 Absolute isotope abundance ratio and atomic weight of a reference sample of Gallium. **J. Res.**  
25 500 **Natl. Bur. Stand.** **91**, 323–331.  
26 501  
27 502 **Mantoura S. (2006)**  
28 503 Development and Application of Opal Based Paleooceanographic Proxies. **PhD Thesis**,  
29 504 **University of Cambridge**, 204 p.  
30 505  
31 506 **Maréchal C.N., Télouk P. and Albarède F. (1999)**  
32 507 Precise analysis of copper and zinc isotopic compositions by plasma-source mass  
33 508 spectrometry **Chemical Geology**, **156**, 251-273.  
34 509  
35 510 **Meija J., Yang L., Sturgeon R., Mester Z. (2009)**  
36 511 Mass Bias Fractionation Laws for Multi-Collector ICPMS: Assumptions and Their  
37 512 Experimental Verification. **Analytical Chemistry**, **81**, 6774-6778.  
38 513  
39 514  
40 515 **Moynier F., Blichert-Toft J., Telouk P., Luck J.M. and Albarède F. (2007)**  
41 516 Comparative stable isotope geochemistry of Ni, Cu, Zn, and Fe in chondrites and iron  
42 517 meteorites **Geochimica et Cosmochimica Acta**, **71**, 4365-4379.  
43 518  
44 519 **Rosman K.J.R. and Taylor P.D.P. (1998)**  
45 520 Isotopic composition of the elements 1997 **Pure & Appl. Chem**, **70**, pp. 217-235.  
46 521  
47 522 **Rouxel O., Escoube R. and Donard O.F.X. (2008)**  
48 523 Measurement of Germanium isotope composition in marine samples by hydride generation  
49 524 coupled to MC-ICP-MS **Geochim. Cosmochim. Acta**, **72**, (12S) A809.  
50 525  
51 526 **Rouxel O., Fouquet Y. and Ludden J.N. (2004)**  
52 527 Subsurface processes at the Lucky Strike hydrothermal field, Mid-Atlantic Ridge; evidence  
53 528 from sulfur, selenium, and iron isotopes **Geochimica et Cosmochimica Acta**, **68**, 2295-2311.



- 1  
2  
3 529  
4 530 **Rouxel O., Galy A. and Elderfield H. (2006)**  
5 531 Germanium isotopic variations in igneous rocks and marine sediments **Geochimica et**  
6 532 **Cosmochimica Acta, 70**, 3387-3400.  
7 533  
8 534  
9 534 **Shima M. (1964)**  
10 535 The distribution of germanium and tin in meteorites **Geochimica et Cosmochimica Acta, 28,**  
11 536 517-532.  
12 537  
13 538  
14 538 **Siebert C., Nägler T.F. and Kramers J.D. (2001)**  
15 539 Determination of molybdenum isotope fractionation by double-spike multicollector  
16 540 inductively coupled plasma mass spectrometry **Geochemistry, Geophysics, Geosystems, 2,**  
17 541  
18 542  
19 542 **Siebert C., Ross A. and McManus J. (2006)**  
20 543 Germanium isotope measurements of high-temperature geothermal fluids using double-spike  
21 544 hydride generation MC-ICP-MS **Geochimica et Cosmochimica Acta, 70**, 3986-3995.  
22 545  
23 546 **Yang L. and Meija J. (2010)**  
24 547 Resolving the germanium atomic weight disparity using multicollector ICPMS **Analytical**  
25 548 **Chemistry, 82**, 4188-4193.  
26 549  
27 549  
28 550  
29  
30  
31  
32  
33  
34  
35  
36  
37  
38  
39  
40  
41  
42  
43  
44  
45  
46  
47  
48  
49  
50  
51  
52  
53  
54  
55  
56  
57  
58  
59  
60

1  
2  
3  
4  
5  
6  
7  
8  
9  
10  
11  
12  
13  
14  
15  
16  
17  
18  
19  
20  
21  
22  
23  
24  
25  
26  
27  
28  
29  
30  
31  
32  
33  
34  
35  
36  
37  
38  
39  
40  
41  
42  
43  
44  
45  
46  
47  
48  
49  
50  
51  
52  
53  
54  
55  
56  
57  
58  
59  
60

Table 1

Name	$^{74}\text{Ge}/^{70}\text{Ge}$	2s	$^{73}\text{Ge}/^{70}\text{Ge}$	2s	$^{72}\text{Ge}/^{70}\text{Ge}$	2s
DS ( $^{70}\text{Ge}$ , $^{73}\text{Ge}$ )	0.07614	0.00010	0.60707	0.00008	0.05626	0.00008
NIST3120a	1.76094	0.00005	0.37335	0.00003	1.32901	0.00004

For Review Only

Table 2

Lab	Method	nb#	$\delta^{74/70}\text{Ge}$ vs. NIST3120a	2s	$\delta^{73/70}\text{Ge}$ vs. NIST3120a	2s	$\delta^{72/70}\text{Ge}$ vs. NIST3120a	2s	$\delta^{74/72}\text{Ge}$ vs. NIST3120a	2s	
<i>"ARISTAR" standard</i>			<u>-0.64</u>	<u>0.18</u>	<u>-0.54</u>	<u>0.18</u>	<u>-0.38</u>	<u>0.26</u>	<u>-0.28</u>	<u>0.03</u>	
#1	HG	SSB	11	-0.58	0.12	nd	-0.30	0.09	-0.28	0.04	
#1	HG	Ga	11	-0.57	0.08	nd	-0.30	0.05	-0.28	0.07	
#2	SiS	SSB	4	-0.59	0.02	-0.47	0.04	-0.33	0.01	-0.26	0.01
#2	SiS	DS	4	-0.61	0.11	-0.46	0.08	-0.31	0.06	-0.30	0.06
#3	SiS	Ga	6	-0.76	0.28	-0.61	0.20	-0.41	0.17	nd	
#3	SiS	SSB	6	-0.75	0.28	-0.63	0.20	-0.63	0.17	nd	
<i>"JMC" standard</i>			<u>-0.32</u>	<u>0.10</u>	<u>-0.23</u>	<u>0.12</u>	<u>-0.16</u>	<u>0.07</u>	<u>-0.16</u>	<u>0.05</u>	
#1	HG	SSB	4	-0.33	0.33	nd	-0.15	0.27	-0.18	0.06	
#1	HG	Ga	4	-0.31	0.29	nd	-0.14	0.25	-0.17	0.06	
#2	SiS	SSB	4	-0.23	0.02	-0.14	0.04	-0.11	0.03	-0.12	0.03
#2	SiS	DS	4	-0.32	0.07	-0.24	0.05	-0.16	0.04	-0.16	0.04
#3	SiS	Ga	8	-0.37	0.04	-0.25	0.02	-0.19	0.07	nd	
#3	SiS	SSB	8	-0.37	0.16	-0.28	0.14	-0.20	0.06	nd	
<i>"SPEX" standard</i>			<u>-0.71</u>	<u>0.21</u>	<u>-0.56</u>	<u>0.15</u>	<u>-0.37</u>	<u>0.16</u>	<u>-0.31</u>	<u>0.08</u>	
#1	HG	SSB	1	-0.59	nd	nd	-0.28	nd	-0.31	nd	
#1	HG	Ga	1	-0.60	nd	nd	-0.28	nd	-0.31	nd	
#1	HG	SSB	5	-0.84	0.16	nd	-0.48	0.10	-0.36	0.08	
#1	HG	Ga	5	-0.81	0.11	nd	-0.46	0.09	-0.35	0.04	
#2	SiS	SSB	3	-0.61	0.04	-0.51	0.09	-0.33	0.03	-0.28	0.05
#2	SiS	DS	4	-0.63	0.13	-0.48	0.10	-0.32	0.06	-0.31	0.06
#3	SiS	Ga	10	-0.81	0.19	-0.62	0.24	-0.41	0.11	nd	
#3	SiS	SSB	10	-0.79	0.18	-0.62	0.16	-0.41	0.12	nd	
#4	SiS	SSB	14	-0.64	0.42	nd	nd	0.00	-0.23	0.26	
#4	SiS	Ga	14	-0.79	0.18	nd	nd	0.00	-0.31	0.04	
<i>"ALDRICH" standard</i>			<u>-2.01</u>	<u>0.23</u>	<u>-1.54</u>	<u>0.17</u>	<u>-1.03</u>	<u>0.12</u>	<u>-0.97</u>	<u>0.15</u>	
#2	SiS	SSB	4	-1.88	0.03	-1.46	0.07	-0.97	0.02	-0.92	0.03
#2	SiS	DS	4	-2.14	0.06	-1.61	0.05	-1.08	0.03	-1.05	0.03
#2	HG	DS	6	-1.90	0.10	-1.44	0.08	-0.96	0.05	-0.94	0.05
#3	SiS	Ga	84	-2.08	0.26	-1.61	0.20	-1.08	0.16	nd	
#3	SiS	SSB	84	-2.05	0.22	-1.60	0.20	-1.06	0.14	nd	

Table 3:

Sample Name	Sample Type	SiO <sub>2</sub> % (m/m)	Ge ug/g	$\delta^{74/70}\text{Ge}$	2s	reference	Mean $\delta^{74/70}\text{Ge}$	2s
BHVO-1	Hawaiian	49.9(a)	1.64(a); 1.55(c)	0.55	0.15	(g)	0.55	0.15
BHVO-2	Basalt	49.9(e)	1.53(k)	0.55	0.13	(k)	0.51	0.10
				0.54	0.13	(k)		
				0.52	0.13	(k)		
				0.43	0.19	(h)		
				0.53	0.15	(h)		
BIR-1	Icelandic Basalt	47.96(e), 47.77(a)	1.5(a); 1.45(b); 1.53(b); 1.49(c); 1.52(d); 1.52(i); 1.40(k)	0.74	0.13	(k)	0.62	0.13
				0.60	0.13	(k)		
				0.56	0.30	(h)		
				0.64	0.33	(g)		
				0.57	0.39	(g)		
				0.61	0.04	(i)		
BCR-1	Columbia River Basalt	54.11(e)	1.5(a); 1.42(b); 1.45(c); 1.36(k)	0.65	0.13	(k)	0.55	0.15
				0.54	0.19	(h)		
				0.47	0.39	(h)		
				0.54	0.22	(g)		
DNC-1	Dolerite	47.15(e), 47.04(a)	1.3(a); 1.26(b); 1.28(k)	0.56	0.13	(k)	0.67	0.19
				0.76	0.13	(k)		
				0.74	0.31	(g)		
				0.61	0.42	(g)		
G-2	Granite	69.1(a)	1.14(a); 0.94(b); 1.02(b); 0.92(k)	0.41	0.30	(h)	0.40	0.03
				0.39	0.34	(g)		
GH	Granite	75.8(e)	2.0(a,f); 2.18(c); 1.63(k)	0.74	0.13	(k)	0.68	0.22
				0.74	0.13	(k)		
				0.55	0.28	(g)		
DTS-1	Dunite	40.41(a)	0.88(a); 0.84(c); 0.83(i); 0.75(k)	0.76	0.13	(k)	0.64	0.26
				0.50	0.06	(i)		
				0.65	0.28	(g)		
PCC-1	Peridotite	41.71(a)	0.94(a); 0.82(k)	0.69	0.13	(k)	0.66	0.13
				0.64	0.13	(k)		
				0.59	0.30	(h)		
				0.74	0.13	(g)		
AN-G	Anorthosite	46.3(a)	0.8(a); 0.93(c); 0.84(k)	0.67	0.13	(k)	0.67	0.01
				0.66	0.13	(g)		
<b>Mean Bulk Silicate Earth</b>							<b>0.60</b>	<b>0.18</b>
GL-O	Glauconite	50.9(a)	4.5(a); 4.02(k)	2.49	0.13	(k)	2.44	0.15
				2.34	0.21	(h)		
				2.51	0.55	(g)		
				2.42	0.26	(g)		
IF-G	Iron Formation	41.2(a)	24(a); 22±0.2(f); 21.8(i); 23.06(k)	1.11	0.13	(k)	1.03	0.09
				1.03	0.13	(k)		
				1.01	0.25	(j)		
				1.00	0.27	(j)		
				1.01	0.17	(i)		

Table 4:

Sample Name	Ge ug/g	$\delta^{74/70}\text{Ge}$	2s	source
<i>Iron meteorite</i>				
Odessa (IAB)	288 (a)	0.96	0.07	<i>this study</i>
		0.98	0.09	Luais, 2007
Braunau (IIA)	183	1.47	0.24	Luais, 2007
<i>Navan PbZn deposit (b)</i>				
U12473	12	-3.86	0.25	<i>this study</i>
U12474	12	-3.95	0.22	<i>this study</i>
U12487	4	-3.36	0.27	<i>this study</i>
U12487	6	-2.82	0.28	<i>this study</i>
U12499	28	-4.28	0.14	<i>this study</i>
<i>Sphalerite (St Salvy mine, France)</i>				
62W	453	-1.05	0.15	Luais, 2007
64W	1047	-2.06	0.15	<i>Luais, submitted</i>
<i>Seafloor sulfide deposits (c)</i>				
FL-24-02	40	-3.26	0.15	<i>this study</i>
FL-19-08	45	-3.24	0.16	<i>this study</i>
ALV-2604-5-1A	159	-2.98	0.20	<i>this study</i>
FL-18-03/fond	200	-4.00	0.11	<i>this study</i>

Review Only

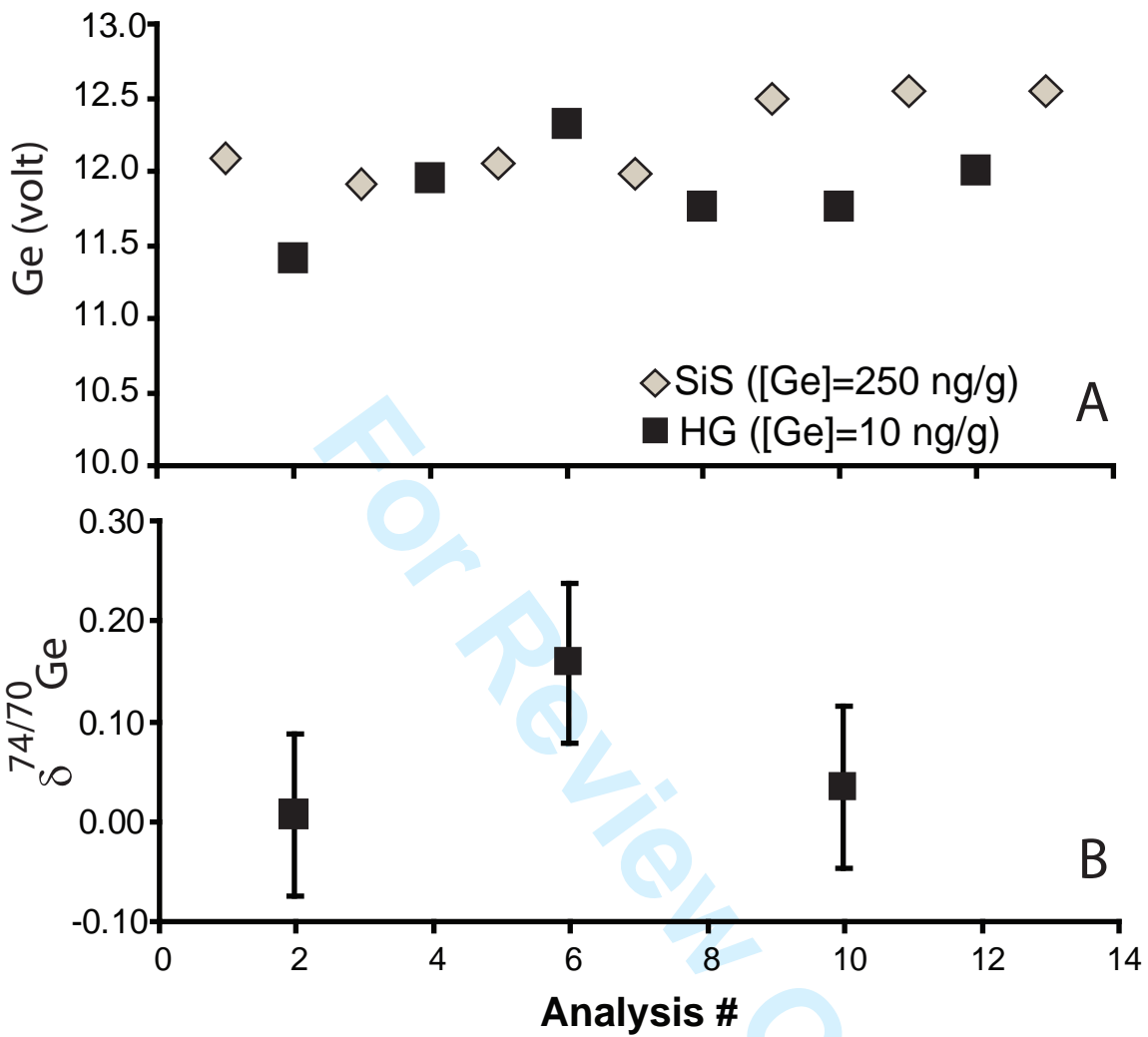


Figure 1

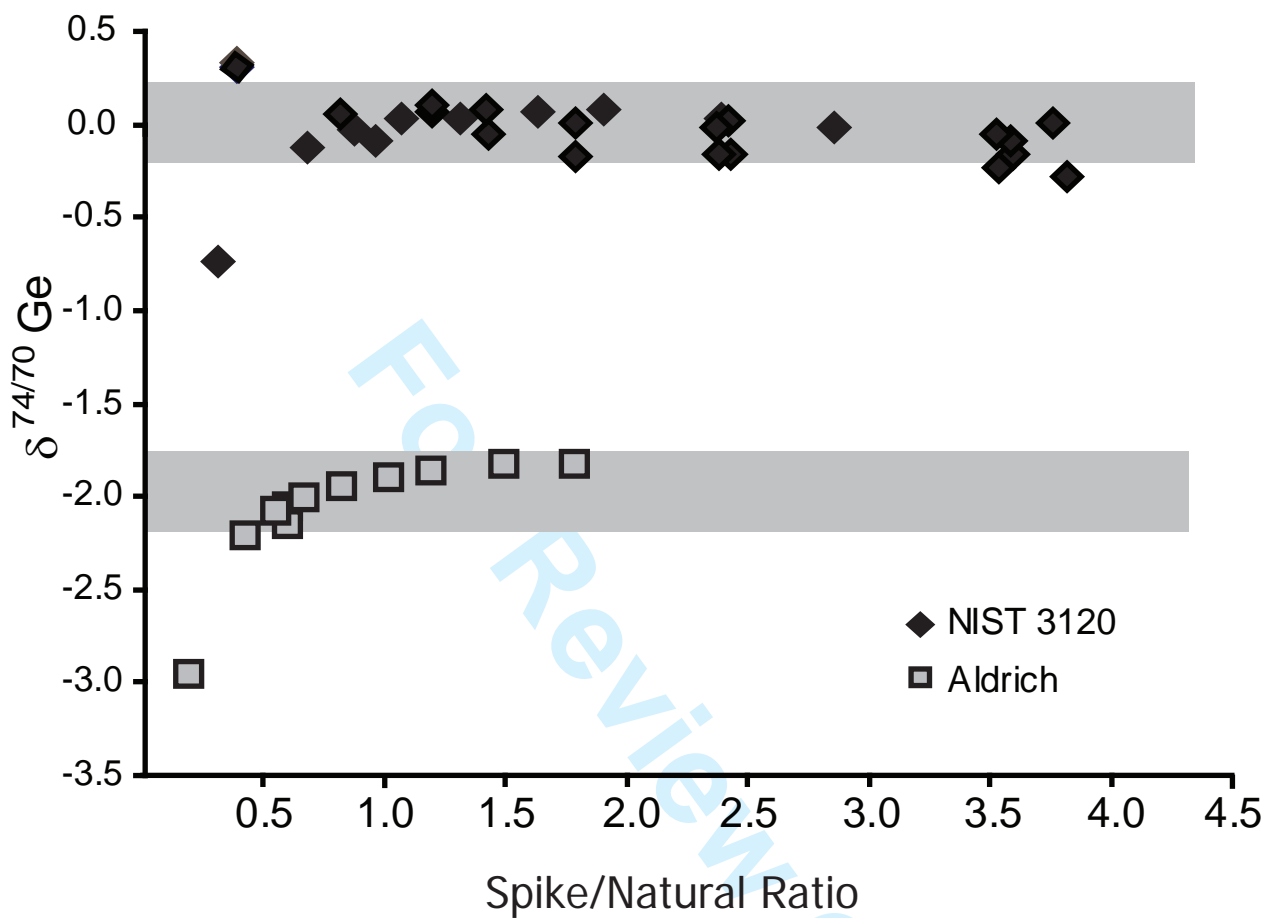


Figure 2

1  
2  
3  
4  
5  
6  
7  
8  
9  
10  
11  
12  
13  
14  
15  
16  
17  
18  
19  
20  
21  
22  
23  
24  
25  
26  
27  
28  
29  
30  
31  
32  
33  
34  
35  
36  
37  
38  
39  
40  
41  
42  
43  
44  
45  
46  
47  
48  
49  
50  
51  
52  
53  
54  
55  
56  
57  
58  
59  
60

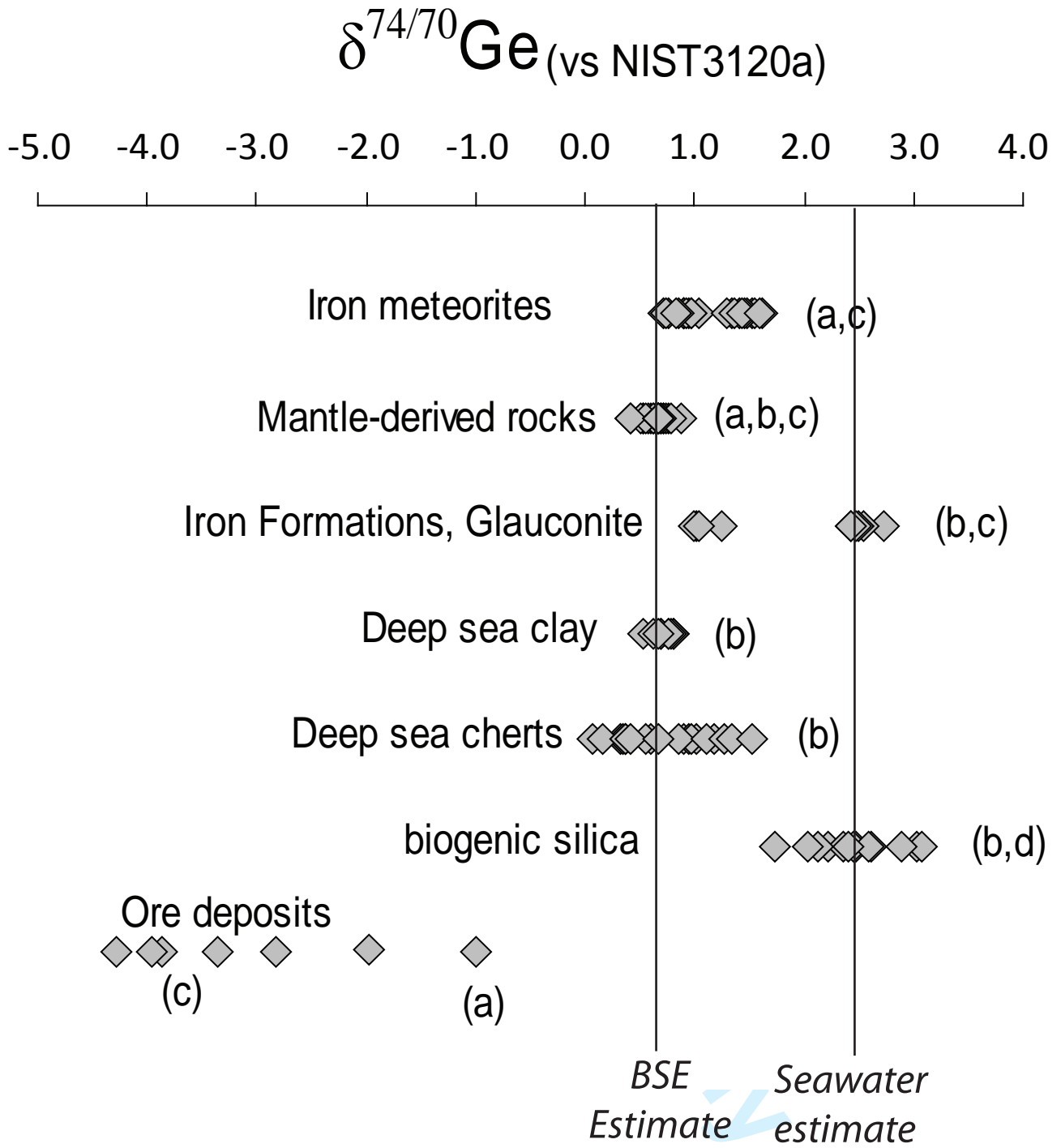


Figure 3